JOURNAL OF PROPULSION AND POWER
Vol. 18, No. 3, May–June 2002

When Do Open-Loop Strategies for Combustion Control Work?

R. K. Prasanth*
Scientific Systems, Inc., Woburn, Massachusetts 01801
A. M. Annaswamy†
Massachusetts Institute of Technology, Cambridge, Massachusetts 02139
J. P. Hathout‡
Robert Bosch Corporation, Palo Alto, CA 9430
and
A. F. Ghoniem§
Massachusetts Institute of Technology, Cambridge, Massachusetts 02139

This paper addresses open-loop control strategies that involve a low-frequency modulation of the fuel injection for suppression of pressure oscillations in combustion systems. Such a strategy has been employed in a number of recent investigations. Using a physically based model, analytical explanations for the effectiveness of such a low pulsing strategy are provided in this paper. Conditions are derived on the frequency and the duty cycle used in the control strategy that lead to stabilization in the combustor, underideal and nonideal switching strategies, and in the presence of hysteresis.

Nomenclature

A_n	=	cross-sectional area of the inlet/outlet
c	=	speed of sound
L	=	length of the combustor
L_n	=	length of the inlet/outlet
p	=	pressure
Q	=	total heat release
S_u	=	burning velocity
T_m	=	pulse period
u	=	axial velocity
V	=	volume of combustor
W_p	=	pulse width
γ	=	specific ratio
Δh_r	=	heat of reaction
ζ	=	passive damping ratio in the combustor
$\eta(t)$	=	modal basis function
$\xi(r, t)$	=	axial displacement of the flame
ρ_u	=	density of the unburnt mixture
τ_c	=	convective delay
τ_f	=	characteristic propagation delay
ϕ	=	equivalence ratio
ϕ_s	=	instantaneous equivalence ratio
$\psi(x)$	=	modal basis function
ω	=	effective Helmholtz frequency
$\bar{(\cdot)}$	=	steady quantity
$(\cdot)'$	=	perturbation quantity

I. Introduction

AN important performance requirement of lean premixed combustion systems is stability over the entire operating range of fuel/airflow. Unstable pressure oscillations are undesirable as they impact the component lifetime and the overall turbine in general. Avoiding unstable operating conditions by increasing the equivalence ratio negatively affects other desirable performance specifications such as low NO_x and high efficiency.

Combustion instability has been observed in systems such as afterburners, gas turbines, and waste incinerators. Practical solutions to avoid it include changes in the acoustic parameters and/or the combustion stabilization mechanisms as well as the use of dampers. Lack of understanding of the underlying mechanisms, models that can predict the instability characteristics as a function of the system geometry, design and operating conditions make it difficult to design stable systems without the use of numerous iterations.

Active control technologies have been explored over the past decade in an effort to combat the unstable dynamics without requiring major hardware redesigns, limiting the operability regime of the engine, or shifting the operating condition away from the state of lowest emission in lean systems or highest power density in near stoichiometric systems. Five different methods have been adopted for active control: 1) phase-shift control, which consists of filtering, phase shifting, and feeding back the pressure signal[1–8]; 2) model-based control, which consists of developing a physically based model of the combustion dynamics has been demonstrated to yield an optimal stabilizing response under certain conditions[9–12]; 3) observer-based control,[13] which has been shown to result in satisfactory pressure suppression using an on-line determination of an observer and a phase-shift controller based on the observer parameters; 4) control based on system-identification-based modeling[14,15]; and 5) open-loop control strategies,[16–21] where the mass flow rate of a fuel injector (and therefore the equivalence ratio) is switched between two different values at a significantly slower frequency than the resonant frequency. This paper concerns analytical discussions of the last method just listed.

Richards et al.[16–18] used a low-frequency pulsing strategy to stabilize the pressure oscillations with no feedback. A similar low-frequency modulation was used by Brouwer et al.[19] The presence of hysteresis in the combustor was used by Knoop et al.[20] and Isella et al.[21] to design a low-frequency pulsing strategy to suppress the pressure oscillations. A 20-kW gas-turbine combustor with a resonant frequency of 300 Hz and an equivalence ratio of 0.85, was stabilized in Richards et al.[16] using a fuel-injector oscillated at 50 Hz and at duty cycles between 0.36 and 0.5. It was also observed that for larger duty cycles (than 0.6) the same injector led to oscillations of a

Received 11 December 2000; revision received 2 October 2001; accepted for publication 20 October 2001.

*Research Engineer.
†Principal Research Scientist, Department of Mechanical Engineering. Member AIAA.
‡Senior Systems Engineer. Member AIAA.
§Professor, Department of Mechanical Engineering, 77 Massachusetts Avenue. Member AIAA.

higher amplitude than without control. The switching strategy was used in a similar rig,[17] but with different switching frequency and duty cycle at different operating conditions. It was shown that the 300-Hz oscillations are reduced significantly by switching between equivalence ratios of 0.65 and 0.75 and an airflow rate of 20.7 g/s, for all switching frequencies less than 20 Hz and duty cycles close to 0.5. The hypothesis proposed in Richards et al.[17] for why stabilization occurs was that these two values of the equivalence ratio correspond to "stable" operating points, and therefore stabilization occurs by switching between these two stable values although the intermediate value of $\phi = 0.7$ corresponds to an "unstable" operating point. Practical considerations of deployment of fuel injectors, in terms of their number as well as location that generate such stable operating points, were discussed by Richards.[18]

The question that arises is: Why does such an open-loop control strategy work? What are the limits of operation of such a methodology? Given that low-frequency pulsing is an attractive method because it circumvents the constraints caused by the currently available bandwidth of available fuel injectors, what are the guidelines for fuel-injector pulsing strategy as well as fuel-injector design in terms of number and location for optimal pressure suppression? If hysteresis is indeed present in a combustor, what are the guidelines for designing a switching strategy? We will attempt to answer these questions in this paper.

II. Analytical Model

In this section we model the combustion dynamics by deriving models of heat release, acoustics and inhomogeneity dynamics, and the coupling dynamics.

A. Heat-Release Dynamics

At high Damkohler numbers and weak-to-moderate turbulence intensity, turbulent combustion can be modeled using wrinkled laminar flames.[22,23] Incorporating the effects of perturbations in the equivalence ratio, the flame surface can be described by a single-valued function $\xi(r, t)$, and the total heat release Q is proportional to the integral of this surface over an anchoring ring. These relations are given by

$$\frac{\partial \xi}{\partial t} = u - v\frac{\partial \xi}{\partial r} - S_u(\phi)\sqrt{\left(\frac{\partial \xi}{\partial r}\right)^2 + 1} \tag{1}$$

$$Q = \kappa(\phi)\int_0^R \sqrt{1 + \left(\frac{\partial \xi}{\partial r}\right)^2}\,\mathrm{d}r \tag{2}$$

with S_u as the burning velocity Δh_r as the heat of reaction being a function of ϕ; $\kappa(\phi) = 2\pi\rho_u S_u(\phi)\Delta h_r(\phi)$; and ρ_u as the density of the unburnt mixture. To derive a linear model, the effects of perturbations in both u and ϕ will be considered.

Assuming negligible velocity component in the radial direction and linearizing around nominal values $\bar{u}$, $\bar{S}_u$, and $\bar{\xi}(r)$ and denoting $(\bar{\cdot})$ and $(\cdot)'$ as steady and perturbation, respectively, we can derive the following linear model[24]:

$$\dot{Q}' = d_0 u' + d_1\left[u'_{\tau_f}(t)\right] + d_2\left[\phi'_{\tau_f}(t)\right] + d_3\phi' + d_\phi\dot{\phi}' \tag{3}$$

where

$$x_\tau(t) \triangleq \int_{t-\tau}^{t} x(\zeta)\,\mathrm{d}\zeta, \qquad \tau_f = \frac{R}{\bar{S}_u}$$

the coefficients d_i depend on S_u and ϕ, and τ_f represents the characteristic propagation delay of the flame surface into the reactants flow.

B. Acoustics

Combustors exhibit instabilities over a range of frequencies including the Helmholtz mode, the longitudinal, and transverse modes. These represent the acoustic component of the instability or the host oscillator. The equations governing the first two are given by

$$\frac{\mathrm{d}^2 p'}{\mathrm{d}t^2} + 2\zeta\omega\frac{\mathrm{d}p'}{\mathrm{d}t} + \omega^2 p' = \frac{\gamma - 1}{V}\dot{q}'(x, t) \tag{4}$$

$$\frac{\partial^2 p'}{\partial t^2} - \bar{c}^2\frac{\partial^2 p'}{\partial x^2} = (\gamma - 1)\dot{q}'(x, t) \tag{5}$$

In the preceding $\omega = \sqrt{(c_i^2 A_i/L_i V + c_e^2 A_e/L_e V)}$ is the effective Helmholtz frequency[25] associated with a combustor connected to ducts. The passive damping caused by different dissipation sources, for examples, heat loss and friction, is accounted for in the natural damping ratio ζ, and $\bar{c}$ is the mean speed of sound. The same approach can be used for transverse modes as well (for example, screech modes in rockets[26]). In what follows, we assume that flames are localized close to the anchoring plane so that $q'(x, t) = q'(t)\delta(x - x_f)$.

Using an expansion in basis functions for both Eqs. (4) and (5) as

$$p'(x, t) = \bar{p}\sum_{l=0}^{n}\psi_i(x)\eta_i(t) \tag{6}$$

where ψ_0 is a constant because it corresponds to the spatial variation in the bulk mode, $\psi_i(x) = \sin(k_i x + \phi_{i0})$, where $i = 1, \ldots, n$, and k_i and ϕ_{i0} are determined from the boundary conditions. Performing a weighted spatial averaging, the modal amplitudes can be shown to follow[9]

$$\ddot{\eta}_i + 2\zeta\omega_i\dot{\eta}_i + \omega_i^2\eta_i = \sum_{i=1}^{n}\tilde{b}_i\dot{q}'_f \tag{7}$$

where $\tilde{b}_0 = (\gamma - 1)/V$; $\tilde{b}_i = \gamma a_0\psi_i(x_f)/E$ for $i = 1, \ldots, n$;

$$E = \int_0^L \psi_i^2(x)\,\mathrm{d}x$$

γ is the specific ratio; $a_0 = (\gamma - 1)/\gamma\bar{p}$; ζ represents the passive damping ratio in the combustor (Dissipation in a combustor can be caused by heat losses in the flame zone and friction caused by viscous effects.); L is its length; $\omega_0^2 = \sqrt{(A_n/L_n V)}$; V is the volume of the combustor; A_n and L_n are the cross-sectional area and length of the inlet/outlet neck connected to the combustor; and $\omega_i = k_i\bar{c}$ for $i = 1, \ldots, n$. Typically, $\omega_0 \ll \omega_i$ for $i = 1, \ldots, n$.

C. Coupling Dynamics

In the case when a Helmholtz-type resonance is triggered in the combustor, the acoustic velocity is very small, and the possible coupling between heat-release fluctuations and acoustics is through the pressure, which in turn produces perturbations in the equivalence ratio via feedline dynamics.[27] In particular, if either the air- or fuel-flow feeds is choked and the other feed is unchoked, ϕ can fluctuate. The instantaneous equivalence ratio ϕ'_s, when linearized, can be shown to satisfy the relation

$$\phi'_s = -(\bar{\phi}/\bar{u})u'_s \tag{8}$$

In addition, there is a convective delay τ_c caused by transport lag from the supply to the burning plane of the flame, and hence,

$$\phi' = \phi'_s(t - \tau_c) \tag{9}$$

where $\tau_c = L/\bar{u}$ and L is the distance between the supply and the burning plane.

The equivalence ratio perturbations, in turn, can be related to the pressure perturbations in the combustor by considering the momentum conservation in the inlet duct,

$$\frac{\partial u'_i}{\partial t} + \frac{1}{\rho_i}\frac{\partial p_i}{\partial x} = 0 \tag{10}$$

where u_i and p_i denote the velocity and the pressure at the inlet duct, respectively. When the dominant acoustic modes are longitudinal, both perturbations in u and ϕ can induce instability. The coupling between u and p can be determined using the energy conservation equation as

$$\frac{\partial p'}{\partial t} + \gamma \bar{p} \frac{\partial u'}{\partial x} = (\gamma - 1) q' \tag{11}$$

D. Overall Model

Combining the acoustics, heat-release, and convective lag effects, we obtain the following equation:

$$\ddot{\eta}_i + 2\zeta \omega_i \dot{\eta}_i + \omega_i^2 \eta_i = \tilde{b}_i \left\{ d_0 u' + d_1 \left[u'_{\tau_f}(t) \right] + d_2 \left[\phi'_{\tau_f}(t) \right] + d_3 \phi'_s(t - \tau_c) + d_\phi \dot{\phi}'_s(t - \tau_c) \right\} \tag{12}$$

This indicates that two different coupling mechanisms are possible excitations for the acoustics, one resulting from the velocity perturbations u' and the other from equivalence ratio perturbations ϕ'. Equation (12) also indicates that two different time delays τ_f and τ_c can induce these excitations, one arising from propagation effects and the other from convection.

The complete combustion dynamics is therefore determined by Eq. (12) and the coupling relations given by Eqs. (9–11). For ease of exposition, we assume that only one acoustic mode is present, and set $\eta_i = \eta$. If the variations are mainly in u', then Eqs. (11) and (12) can be combined to obtain the relation

$$\ddot{\eta} + 2\zeta_0 \omega_0 \dot{\eta} + \omega_0^2 \eta - \gamma_2 \eta(t - \tau_f) = 0 \tag{13}$$

where

$$2\zeta_0 \omega_0 = 2\zeta\omega - \gamma_1, \qquad \omega_0^2 = \omega^2 + \gamma_2, \qquad \gamma_1 = \frac{R}{\bar{S}_u}\gamma_2$$

$$\gamma_2 = \bar{\kappa} \bar{S}_u \frac{\bar{p} a_0}{E k^2} \left[\frac{\mathrm{d}\psi}{\mathrm{d}x} \psi(x) \right]_{x_f}, \qquad \tau_f = \frac{R}{\bar{S}_u} \tag{14}$$

and if they are caused by ϕ' then Eqs. (9), (10), and (12) can be combined to obtain

$$\ddot{\eta} + 2\zeta\omega\ddot{\eta} + \omega_i^2 \dot{\eta} - \beta_1 \dot{\eta}(t - \tau_c) + \beta_2 \eta(t - \tau_c) - \beta_3 \eta_{fc}(t) = 0$$

$$\eta_{fc} = \int_{t - \tau_f - \tau_c}^{t - \tau_f} \eta(\zeta)\, \mathrm{d}\zeta \tag{15}$$

where

$$\beta_1 = 2\pi \tilde{b} \frac{\bar{\phi}}{\bar{u}} \tilde{c} \gamma k^2 \left(\bar{S}_u \left. \frac{\mathrm{d}\Delta h_r}{\mathrm{d}\phi} \right|_{\bar{\phi}} + \Delta \bar{h}_r \left. \frac{\mathrm{d}\bar{S}_u}{\mathrm{d}\phi} \right|_{\bar{\phi}} \right) \left(\int_0^R \bar{\xi}\, \mathrm{d}r \right)$$

$$\beta_2 = 2\pi \tilde{b} \frac{\bar{\phi}}{\bar{u}} \tilde{c} \gamma k^2 \Delta \bar{h}_r \bar{S}_u \frac{\mathrm{d}\bar{S}_u}{\mathrm{d}\phi} \bar{\xi}(0)$$

$$\beta_3 = -2\pi \Delta \bar{h}_r \tilde{b} \frac{\bar{\phi}}{\bar{u}} \tilde{c} \gamma k^2 \bar{S}_u^2 \frac{\mathrm{d}\bar{S}_u}{\mathrm{d}\phi} \left. \frac{\mathrm{d}\bar{\xi}}{\mathrm{d}r} \right|_0, \qquad \tau_c = \frac{L}{\bar{u}}$$

At the acoustic frequency, the impact of the fifth and sixth term on the left-hand side of Eq. (15) is typically smaller. Also τ_f is small compared to τ_c in many cases. Hence a simplified version of Eq. (15) can be analyzed in the form

$$\ddot{\eta} + 2\zeta\omega\dot{\eta} + \omega^2 \eta - \beta_1 \eta(t - \tau_c) = 0 \tag{16}$$

The structure of Eq. (16) is identical to that of Eq. (13) with the differences only caused by the parameters. This implies that time-delay effects are present both in the presence of u' and ϕ' perturbations, with the distinction that with u', the time delay is caused by τ_f, which is caused by flame propagation, and with ϕ', the delay is caused by τ_c, a convection effect. The other distinction is in the damping effect; in the former, if γ_1 is positive, even in the absence of any time delay, instabilities can be present. In the latter, on the other hand, instability is only caused by the time delay τ_c; the damping effect is stabilizing.

E. Discussion

The models in Eqs. (13) and (16) were discussed at length in Hathout et al.,[24] and were shown to exhibit intervals of alternating stable and unstable behavior as the time delay increased. These models were also shown to predict the instability behavior of a number of experimental rigs. In particular, the model in Eq. (16) was shown to alternate between stability and instability as the convective lag τ_c increased, which was similar to the properties of the rig considered in Richards et al.[16] Similarly, the model in Eq. (13) appears to match the stability map in Fig. 6 in Richards et al.[17] which shows the stability bands.

A few comments about the various parameters in Eqs. (13) and (16) are in order. We discuss the parameters in Eq. (13) first. The dependence of γ_i on ϕ is straightforward because of the changes of Δh_r and S_u with ϕ. In general, for values of $\phi \leq 1$, γ_0 and γ_1 increase with ϕ. Similarly, τ_f increases with a decreasing ϕ because of its dependence on S_u for values away from the lean blow out (LBO) limit and unity. The dependence of ω on ϕ is indirect and occurs through the temperature, which increases as ϕ increases and hence increases the speed of sound and therefore the frequency. The quantity ζ_0 depends on the flame position with respect to the acoustic mode. For example, a quarter-wave acoustic mode implies that γ_1 is negative and therefore ζ_0 is positive, and, hence, leads to a stable system for small values of τ_f, and destabilizes as τ_f increases.

The parameters in Eq. (16) are also dependent on $\bar{\phi}$ but to a smaller extent. For example, changes in τ_c are more likely to occur with changes in the mean velocity $\bar{u}$ rather than $\bar{\phi}$. Even though the parameter β_1 changes with S_u and Δh_r as ϕ increases because it occurs as a linear coefficient in Eq. (16), its changes do not produce drastic differences in the stability characteristics of Eq. (16). The damping coefficient is unchanged with flame position, whereas the frequency dependence with ϕ is the same as in Eq. (13) because of temperature changes.

III. Stabilization Using the Open-Loop Control Strategy

In this section we address the problem of stabilization using an open-loop control strategy that consists of switching between two values of equivalence ratio. In particular, we will focus on the strategies used in Richards et al.[16,17] which consist of changing the equivalence ratio between two constant values at a frequency that is significantly lower than the resonant frequency. The discussions in the preceding section indicate that while the specific dependence of the individual parameters might be different, the general class of models that describe the combustion instability is of the form

$$\ddot{\eta} + 2\zeta_0 \omega \dot{\eta} + (\omega^2 - k_1)\eta + k_2 \eta(t - \tau) = 0 \tag{17}$$

with the exact variations in $\zeta_0, \omega, k_1, k_2$, and τ depending on whether the instability is caused by u' or ϕ'. Using the model in Eq. (17), we derive the conditions under which the switching strategy can stabilize the combustion dynamics. Design procedures for meeting these stabilization conditions are also discussed.

A. Ideal Switching

The control strategy in Richards et al.[16,17] can be described as follows: Starting from $t_0 = 0$, define $t_i = t_{i-1} + T_m$ for $i \geq 1$ and modulate equivalence ratio according to

$$\phi(t) = \begin{cases} \phi_1 & \text{for} \quad t_{i-1} \leq t < t_{i-1} + W_p T_m \\ \phi_2 & \text{for} \quad t_{i-1} + W_p T_m \leq t < t_i \end{cases} \tag{18}$$

where $0 \leq W_p \leq 1$ is the pulse width and T_m is the pulse period. The parameters $(\omega, \zeta_0, k_1, k_2, \tau)$ of the model (17) are functions of ϕ, and under this ideal switching strategy the system (17) becomes

a time-varying time-delay system. Our objective is to analyze the stability of this system and derive conditions from which the design variables (ϕ_1, ϕ_2, W_p, T_m) can be computed readily.

Let us rewrite Eq. (17) in the following way:

$$\ddot{\eta} + 2\zeta_\phi \omega_\phi \dot{\eta} + \left(\omega_\phi^2 - k_{1\phi}\right)\eta + \alpha_{1\phi}\eta\left(t - \tau_{\phi_1}\right) + \alpha_{2\phi}\eta\left(t - \tau_{\phi_2}\right) = 0 \tag{19}$$

where subscripts have been introduced to show dependence of the parameters on equivalence ratio ϕ. We have also brought in two new functions $\alpha_{1\phi}$ and $\alpha_{2\phi}$ that switch according to

$$\alpha_{k\phi} = \begin{cases} k_{2\phi_k} & \text{if} \quad \phi = \phi_k \\ 0 & \text{otherwise} \end{cases}$$

The procedure outlined next establishes, in a rigorous manner, that the system in Eq. (19) can be stabilized using a large enough T_m provided that there are two operating points with equivalence ratios ϕ_1 and ϕ_2 on either side of the desired unstable operating point with at least one of them being stable. Once this is established, the question that remains is to determine the conditions under which such a stability pattern exists in a given rig. In particular, we note that the stability of the system in Eq. (19) is dependent on the parameter values of $f(\phi)$, where

$$f(\phi) = (\omega_\phi, \zeta_\phi, k_{1\phi}, \alpha_{1\alpha}, \alpha_{2\phi}, \tau_\phi) \tag{20}$$

which obviously changes with ϕ. This dependence is discussed in Sec. VI.

1. *Stability Conditions Under Ideal Switching*

It is clear that Eq. (19) describes Eq. (17) under the control strategy (18). When ϕ is a constant, the system (19) can be written in feedback interconnection form as

$$\hat{y} = \frac{s+1}{\left[s^2 + 2\zeta_\phi\omega_\phi s + \left(\omega_\phi^2 - k_{1\phi}\right)\right]} u = (s+1)G_\phi(s)u \tag{21}$$

$$u = -\frac{1}{s+1}\begin{bmatrix} e^{-\tau_{\phi_1} s} & e^{-\tau_{\phi_2} s} \end{bmatrix}\begin{bmatrix} \alpha_{1\phi} \\ \alpha_{2\phi} \end{bmatrix}\hat{y} = D(s)\alpha_\phi \hat{y} \tag{22}$$

$$\eta = y \tag{23}$$

where the infinite dimensional component D is time invariant. This feedback interconnection is shown on the left of Fig. 1. The block diagram shows that we have simply added a stable pole and a canceling minimum phase zero in order to generate a finite dimensional uniform approximation.

Now, given any $\gamma > 0$ there exists a finite dimensional system P with a rational transfer function of degree say $2n$ such that

$$P + \Delta = D(s) = 1/(s+1)\begin{bmatrix} e^{-\tau_{\phi_1} s} & e^{-\tau_{\phi_2} s} \end{bmatrix} \tag{24}$$

where the approximation error Δ satisfies

$$|\Delta(j\omega)| \leq 1/\gamma$$

for all frequency ω including ∞. Similarly, given any order n, we can compute a system P of order n and a number $\gamma > 0$ such that the approximation error is smaller in magnitude than $1/\gamma$ at every frequency. Moreover, as n goes to infinity the approximation error goes to zero uniformly. This additive representation of the infinite dimensional part of Eq. (19) is shown on the right-hand side of Fig. 1. The system within the dashed line is the approximate system of degree $2n+2$ that we shall work with. This system has a scalar output z and a 2×1 vector input w with state-space realization

$$\dot{x}_g = \begin{bmatrix} 0 & 1 \\ -\left(\omega_\phi^2 - k_{1\phi}\right) & -2\zeta_\phi\omega_\phi \end{bmatrix} x_g + \begin{bmatrix} 0 \\ 1 \end{bmatrix}\hat{u} = A_\phi x + B_g \hat{u} \tag{25}$$

$$\hat{y} = [1 \quad 1]\, x_g = C_g x_g \tag{26}$$

for $(s+1)G_\phi$, and a realization

$$\dot{x}_p = A_p x_p + B_p z \tag{27}$$

$$\hat{w} = C_p x_p \tag{28}$$

for P. Combining these two state-space models, we arrive at the following realization for the approximate system:

$$\dot{x} = \begin{bmatrix} A_\phi & B_g C_p \\ -B_p \alpha_\phi C_g & A_p \end{bmatrix} x + \begin{bmatrix} B_g \\ 0 \end{bmatrix} w = \hat{A}_\phi x + Bw \tag{29}$$

$$z = [-\alpha_\phi C_g \quad 0]\, x = C_\phi x \tag{30}$$

where $x = [x_g^T, x_p^T]^T$. When ϕ is modulated according to Eq. (18), Eqs. (29) and (30) describe a finite dimensional linear time-varying system.

We now describe the design procedure for choosing W_p and T_m in Eq. (18) so as to stabilize Eq. (19). This is done in the following two steps. In the first step, we describe how W_p and T_m can be chosen so that Eq. (18) stabilizes Eqs. (29) and (30). In the second step, we derive additional conditions that need to be satisfied by W_p and T_m so that Eq. (18) stabilizes the actual system in Eq. (19).

The following lemma provides the conditions for stabilization of Eqs. (29) and (30) using Eq. (18).

Lemma 1: The system in Eqs. (29) and (30) with the control strategy (18) is asymptotically stable if and only if there exists a periodic (with period T_m), positive definite function P such that

$$\dot{P} + \hat{A}_\phi^T P + P\hat{A}_\phi < 0 \tag{31}$$

for all $t \leq 0$.

The design procedure consists of choosing W_p and T_m so that Eq. (31) is satisfied for some P and so that

$$\phi_{\text{av}} = W_p\phi_1 + (1 - W_p)\phi_2 \tag{32}$$

where ϕ_{av} is the desired operating condition. Given a ϕ_{av}, once stable operating points ϕ_1 and ϕ_2 are found such that $\phi_1 < \phi_{\text{av}} < \phi_2$, Eq. (32) determines W_p. Therefore, what remains is to show how T_m can be chosen so that Eq. (31) is satisfied.

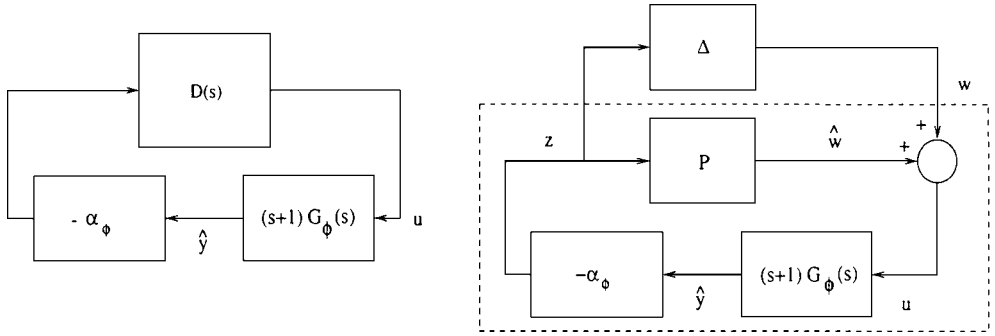

Fig. 1 Block diagram for approximation procedure.

To determine T_m from Eq. (31), fix T_m, and subdivide the time interval $[0, T_m]$ into M equal parts, $0 < \epsilon < 2\epsilon < \cdots < M\epsilon = T_m$. Let us denote by $\dot{P}_k$, P_k, $\hat{A}_k$, and C_k the values of $\dot{P}$, P, $\hat{A}_\phi$, and C_ϕ respectively at time $k\epsilon$ Now, if the subdivision is suffciently fine (or if $\dot{P}$ is piecewise linear) then

$$P_k = P_0 + \frac{\epsilon}{2}\left(\dot{P}_0 + \dot{P}_k + 2\sum_{j=1}^{k-1}\dot{P}_j\right) \tag{33}$$

for $k \geq 1$. Periodicity of P implies that $P_0 = P_M$. This, along with Eq. (33) at $k = M$ and the periodicity of $\dot{P}$ gives

$$\dot{P}_0 = \dot{P}_M = -\sum_{k=1}^{M-1}\dot{P}_k \tag{34}$$

Using the preceding developments, the linear matrix inequality (LMI) conditions in lemma 1 can be replaced by the finite set of sufficient LMIs:

$$P_0 > 0 \tag{35}$$

$$P_k = P_0 + \frac{\epsilon}{2}\left(\dot{P}_0 + 2\sum_{j=1}^{k-1}\dot{P}_j + \dot{P}_k\right) > 0 \tag{36}$$

$$-\left(\sum_{m=1}^{M-1}\dot{P}_m\right) + \hat{A}_0^T P_0 + P_0\hat{A}_0 < 0 \tag{37}$$

$$\dot{P}_k + \hat{A}_k^T P_k + P_k\hat{A}_k < 0 \tag{38}$$

where $k = 1, 2, \ldots, M-1$. Here, the unknowns are $(P_0, \dot{P}_1, \ldots, \dot{P}_{M-1})$. These matrices can be computed using efficient numerical techniques that have been developed in the LMI literature[28] (for example, the MATLAB® LMI toolbox).

We now show that Eq. (18) stabilizes the original system (19) if T_m is chosen so that P satisfies a linear matrix inequality that is somewhat stronger than Eq. (31). Noting that the difference between the approximate and actual system is represented by Δ, it follows that if D can admit perturbations large enough compared to Δ, then stabilization of the actual system is possible. This is stated more formally in the following two lemmas .

Let $\mathcal{L}_2$ denote the Hilbert space of functions of time with finite energy. Roughly speaking, a function f is in $\mathcal{L}_2$ if and only if

$$\int_0^\infty f(t)^T f(t)\,\mathrm{d}t < \infty$$

We can view the approximate system with input w and output z in Fig. 1 as a mapping from $\mathcal{L}_2$ into $\mathcal{L}_2$. For each input w of finite energy, the system generates an output z whose energy is scaled by a factor. The largest scaling factor, obtained by searching over all finite energy inputs, is called the *induced norm* of the system. The following lemma gives a sufficient condition for stability of the original system and is an application of the small gain theorem.[29]

Lemma 2: Let $\gamma > 0$ be given, P be the corresponding uniform approximation defined in Eq. (24), and the equivalence ratio ϕ satisfy the control law (18) for some $(\phi_1, \phi_2, W_p, T_m)$. Suppose that the induced norm of the time-varying system from w to z in Fig. 1 is strictly less than γ. Then, the infinite dimensional system (19) with the control law (18) is stable.

The preceding lemma suggests that the design variables $(\phi_1, \phi_2, W_p, T_m)$ are to be selected so that the induced norm of the approximate system satisfies a specified bound. Such an induced norm can be guaranteed to exist if an LMI condition that is similar to that in Eq. (31), and somewhat stronger, is satisfied. This is stated in the following lemma.

Lemma 3: Let $\gamma > 0$ be given. The approximate system (29) and (30) with the control strategy (18) has induced norm strictly less than γ if and only if there exists a periodic (with period T_m) positive definite function P such that

$$\begin{bmatrix} \dot{P} + \hat{A}_\phi^T P + P\hat{A}_\phi + C_\phi^T C_\phi & PB \\ B^T P & -\gamma^2 I \end{bmatrix} < 0 \tag{39}$$

for all $t \geq 0$.

2. *Control Design Procedure*

The summary of Lemmas 1 and 3 is the following: The switching strategy in Eq. (18) is guaranteed to stabilize the combustion instability model in Eq. (19) if a certain LMI condition is satisfied. The question that arises is if indeed this condition is satisfied for a given combustion system. In particular, given a desired operating condition ϕ_{av} and values ϕ_1 and ϕ_2 that are $\phi_1 < \phi_{\text{av}} < \phi_2$, the problem is to determine the design procedure for calculating T_m such that the LMI condition (39) can be satisfied. We address this question by considering the following three cases: 1) stable-stable switching (This case corresponds to the behavior of the combustor considered in Richards et al.[17] near the operating point $\phi_{\text{av}} = 0.7$ with equivalence ratio modulated between two stable points.)—the system (17) is stable at ϕ_1 and ϕ_2; but not necessarily stable at ϕ_{av}; 2) stable-unstable switching (This case corresponds to the combustor behavior discussed in Richards et al.[17] near $\phi_{\text{av}} = 0.9$ with switching between a stable and an unstable point.)—the system (17) is stable at one of the points (say ϕ_1) and unstable at the other (ϕ_2); and 3) unstable-unstable switching—the system (17) is unstable at ϕ_1 and ϕ_2.

Figure 2 illustrates these cases. The function shapes shown are representative of the three cases, but we make no assumption about their exact shape or, more precisely, about the relationship between equivalence ratio and system stability over the entire range of equivalence ratios. The only assumption made is about the stability at the three points ϕ_1, ϕ_{av}, and ϕ_2. In all three cases, ϕ_1 and ϕ_2 must also satisfy $\phi_1 < \phi_{\text{av}} < \phi_2$ so that the time-averaged equivalence ratio can equal ϕ_{av}, that is, Eq. (32) holds for some $0 \leq W_p \leq 1$. These cases are considered in some detail in the following.

a. Stable-stable switching. If ϕ_1 and ϕ_2 are stable operating points and the goal is to switch between these two points and still ensure stability, essentially one needs to switch sufficiently slowly so that any transients that are induced as a result of the switching die down during the switching period. That is, if T_m is large enough, these transients are guaranteed to die down and hence ensure stability. In fact, it can be shown that the LMI conditions in

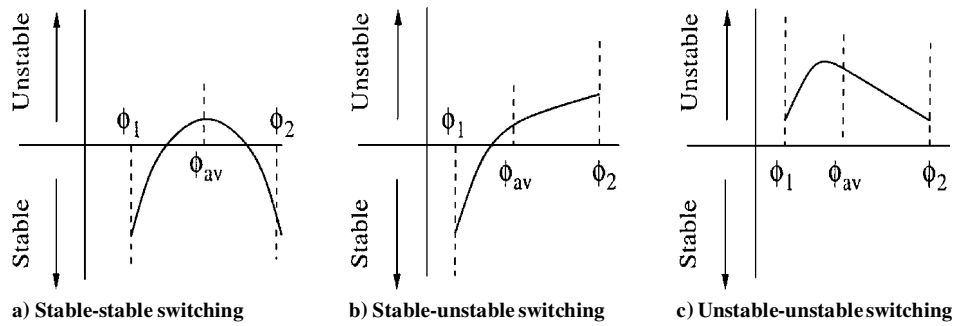

a) Stable-stable switching **b) Stable-unstable switching** **c) Unstable-unstable switching**

Fig. 2 Three switching cases based on stability properties at ϕ_1, ϕ_{av}, and ϕ_2.

Eq. (39) hold for a sufficiently large T_m irrespective of W_p. Because stability in this case is independent of the pulse width W_p, any desired operating equivalence ratio ϕ_{av} between ϕ_1 and ϕ_2 can be achieved by simply choosing W_p according to Eq. (32). A procedure to compute the design parameters is the following:

1) Select ϕ_1 and ϕ_2 such that $\phi_1 \le \phi_{\text{av}} \le \phi_2$ and the system (17) is stable at ϕ_1 and ϕ_2.

2) Choose W_p according to Eq. (32).

3) Choose a large period T_m^{big} and perform bisection between [0, T_m^{big}] until the smallest time period $T_m^{\min}$ for which the LMIs in Eq. (39) hold.

Any $T_m \ge T_m^{\min}$ will result in stability of the controlled system (17).

b. Stable-unstable switching. Unlike case a), "instability" or pressure amplification can result in this case either from switching or because of operating at an unstable point. Therefore, the fraction of time spent at the unstable operating point is relevant to stability of the overall system. That is, stability is determined by both W_p and T_m. As a result, not all ϕ_{av} between ϕ_1 and ϕ_2 can be achieved by switching.

The set of all W_p and T_m (equivalently, ϕ_{av} and T_m) that result in stability of Eq. (17) under the control strategy (18) can be computed as follows:

1) Select ϕ_1 and ϕ_2 such that $\phi_1 \le \phi_{\text{av}} \le \phi_2$ and the system (17) is stable at ϕ_1 and unstable at ϕ_2.

2) Choose a period T_m. Perform bisection on W_p between [0, 1] to determine the smallest $W_p^{\min}$ for which the LMIs in Eq. (39) hold.

3) Repeat step 2) for a different T_m.

For any period $T_m > 0$, the pulse width $W_p = 1$ guarantees stability as it corresponds to operation at the stable point $\phi = \phi_1$. Similarly, $W_p = 0$ results in instability. The bisection in step 2) computes the smallest pulse width needed to guarantee stability for a fixed pulse period T_m. It is clear that large T_m and large W_p (or ϕ_{av} close to ϕ_1) result in stability of the controlled system.

c. Unstable-unstable switching. It is easy to see that large periods result in instability of the original system. Therefore, this case does not fit into the concept of stabilization via low frequency switching. That is, the system cannot be stabilized using the switching strategy in Eq. (18) if ϕ_1 and ϕ_2 correspond to unstable operating points, almost always.

B. Nonideal Switching

The switching strategy given by Eq. (18) assumes that transition between the two equivalence ratios is instantaneous. But, in general, the transition time depends on the actuator bandwidth (i.e., opening and closing times of the injector valve) as well as the time taken for the reaction zone to reach the new equivalence ratio. Consider the following nonideal switching:

$$\phi(t) = \begin{cases} \phi_{\text{av}} & \text{for} \quad t = 0 \\ \hat{\phi}_1(t) & \text{for} \quad 0 \le t < \delta \\ \phi_1 & \text{for} \quad \delta \le t < W_p T_m - \delta \\ \hat{\phi}_2(t - W_p T_m + \delta) & \text{for} \quad W_p T_m - \delta \le t < W_p T_m + \delta \\ \phi_2 & \text{for} \quad W_p T_m + \delta \le t < T_m - \delta \\ \hat{\phi}_3(t - T_m + \delta) & \text{for} \quad T_m - \delta \le t < T_m \\ \phi_{\text{av}} & \text{for} \quad t = T_m \end{cases} \tag{40}$$

where $\delta > 0$ is the transition time, $\hat{\phi}_i$ are continuous functions of time that describe the variation of ϕ during transition periods, and the remaining variables are as before. It turns out that the delay $e^{-\tau_\phi s}$ might not be a bounded operator, and some assumptions are needed to extend the analysis of the preceding section. We assume that the effect of nonideal continuous switching can be approximated by that of a finite number of small ideal switches. In particular,

$$\frac{e^{-\tau_\phi s}}{s+1} \approx \sum_{k=1}^{N} \alpha_{k\phi} \frac{e^{-\tau_k s}}{s+1}$$

for some $\alpha_{k\phi}$ of the form in the preceding section. With this assumption, it can be shown that Eq. (39) gives sufficient conditions for stability of the original system provided that the approximate model (29) and (30) is constructed with N delay terms instead of two as in the preceding section.

To compute W_p and T_m in this nonideal switching case, we proceed as before by first selecting ϕ_1 and ϕ_2 such that $\phi_1 \le \phi_{\text{av}} \le \phi_2$. The stability properties of the system at ϕ_1 and ϕ_2 determine whether we should follow the design procedure for stable-stable or stable-unstable case described in the preceding section. In either case, the computed values of W_p and T_m are guaranteed to stabilize the system only if the delay approximation given above is good. Indeed, δ and the functions $\hat{\phi}_i$ appearing in Eq. (40) strongly influence the quality of approximation. Large transition times and highly nonlinear variation of equivalence ratio during transition will make approximation difficult.

IV. Stabilization in the Presence of Hysteresis

In the preceding section we implicitly assumed that the parameter vector $f(\phi) = (\zeta_\phi, \omega_\phi, k_{1\phi}, k_{2_\phi}, \tau_\phi)$ is single valued at each ϕ. Often a hysteresis mechanism is present in combustion systems.[21] This in turn implies that $f(\phi)$ is multivalued between ϕ_1 and ϕ_2. Interestingly enough, even in this case, stabilization is possible using the same switching strategy as in Eq. (40), with the underlying conditions involving functional forms of $f(\phi)$ for both branches of hysteresis (Fig. 3). To do this, consider the hysteresis cycle shown in Fig. 3, and suppose that the desired operating point is ϕ_{av}. Let us denote the lower and upper halves of hysteresis cycle by f_1 and f_2, respectively. Also, suppose that δ is the transition time between ϕ_1 and ϕ_{av} as well as between ϕ_{av} and ϕ_2. Thus, in the presence of hysteresis switching between ϕ_1 and ϕ_2 leads to combustor parameter variation given by

$$f(\phi)(t) = \begin{cases} f_1(\phi_{\text{av}}) & \text{for} \quad t = 0 \\ f_1[\hat{\phi}_1(t)] & \text{for} \quad 0 \le t < \delta \\ f_1(\phi_1) = f_2(\phi_1) & \text{for} \quad \delta \le t < W_p T_m - \delta \\ f_2[\hat{\phi}_2(t - W_p T_m + \delta)] & \text{for} \quad W_p T_m - \delta \le t < W_p T_m + \delta \\ f_2(\phi_2) = f_1(\phi_2) & \text{for} \quad W_p T_m + \delta \le t < T_m - \delta \\ f_1[\hat{\phi}_3(t - T_m + \delta)] & \text{for} \quad T_m - \delta \le t < T_m \\ f_1(\phi_{\text{av}}) & \text{for} \quad t = T_m \end{cases} \tag{41}$$

which is no more general than the parameter variations generated by the nonideal switching strategy (40). Therefore, Eq. (39) once again corresponds to sufficient conditions for stabilization with the approximate system represented using N delays rather than two, as discussed in the preceding section.

Let us examine some of the consequences of our analytical results for stabilization in the presence of hysteresis. First, there is a minimum value of pulse period T_m below which stabilization is not possible. Intuitively, this is because rapid switching results in very little time for transients to die out. Second, because part of the hysteresis cycle leads to unstable operating condition, pulse width

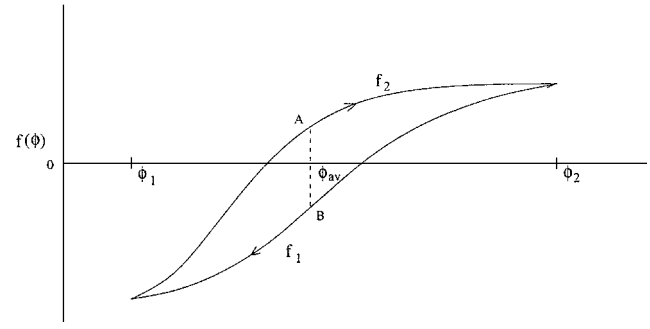

Fig. 3 Hysteresis curve.

cannot be arbitrary for stabilization. This is similar to the stable-unstable switching we considered. A third statement we can make is that because of the nonzero transition time δ, short pulses might not be stabilizing. These statements corroborate the following observations made in Isella et al.[21]: 1) pulsing at a slower frequency than the unstable frequency stabilizes the system, and 2) shorter pulses tend to be less effective, in general.

Recall that ϕ_1 and ϕ_2 are design variables that must be chosen along with W_p and T_m so that Eq. (32) and the LMIs (35–38) hold to guarantee stability. In the presence of hysteresis, an additional condition, which we implicitly assumed, must hold. This condition is the following: ϕ_1 and ϕ_2 must be sufficiently apart so that the lower and upper halves of the hysteresis cycle meet at ϕ_1 and ϕ_2:

$$f_1(\phi_1) = f_2(\phi_1), \qquad f_1(\phi_2) = f_2(\phi_2)$$

To realize a ϕ_1 and ϕ_2 that are far apart, if the air-flow rate is fixed, one would require flow-rates of the secondary-fuel to be sufficiently different at the instances t and $t + T_m$. Hence, at least at one of these instances, the flow rate of the fuel injector should be large enough. This corroborates yet another observation made in Isella et al.[21]: 3) the flow rate needed to accomplish successful pressure suppression is substantial (about 25% of the primary fuel-flow rate). It is quite likely that the primary loop of the hysteresis curve in Knoop et al.[20] and Isella et al.[21] corresponded to an equivalence ratio change that is commensurate with a 25% change in the fuel-flow rate. This discussion shows that Eq. (39) provides sufficient conditions for stabilization with infinite switching in the presence of hysteresis.

When hysteresis is present, a considerably simpler control strategy suffices: a single pulse of sufficient duration and height. This can be explained using Fig. 3. Let us assume that operation begins on the upper half of the hysteresis cycle at an equivalence ratio of ϕ_{av} (point A in Fig. 3). For stabilization using hysteresis, we need a pulse of sufficient duration and height so that the equivalence ratio ϕ_2 can become effective following which the system can return to the desired operating point B in Fig. 3 along the lower branch during the off period. Thus, during this single period the switching strategy takes the equivalence ratio from ϕ_{av} to ϕ_2 and back. As long as the pulse duration and width are large enough to allow transition from ϕ_{av} to ϕ_2, stabilization will occur. This confirms the observations (1–3) made in Isella et al.[21] As with the infinite switching strategy, we note that the robustness of this single pulse strategy is nonexistent; as long as perturbations are present, the operating point will move from B to A causing pulsing to be invoked repeatedly.

This paper does not answer the question regarding how general the existence of hysteresis is in combustors or what the responsible

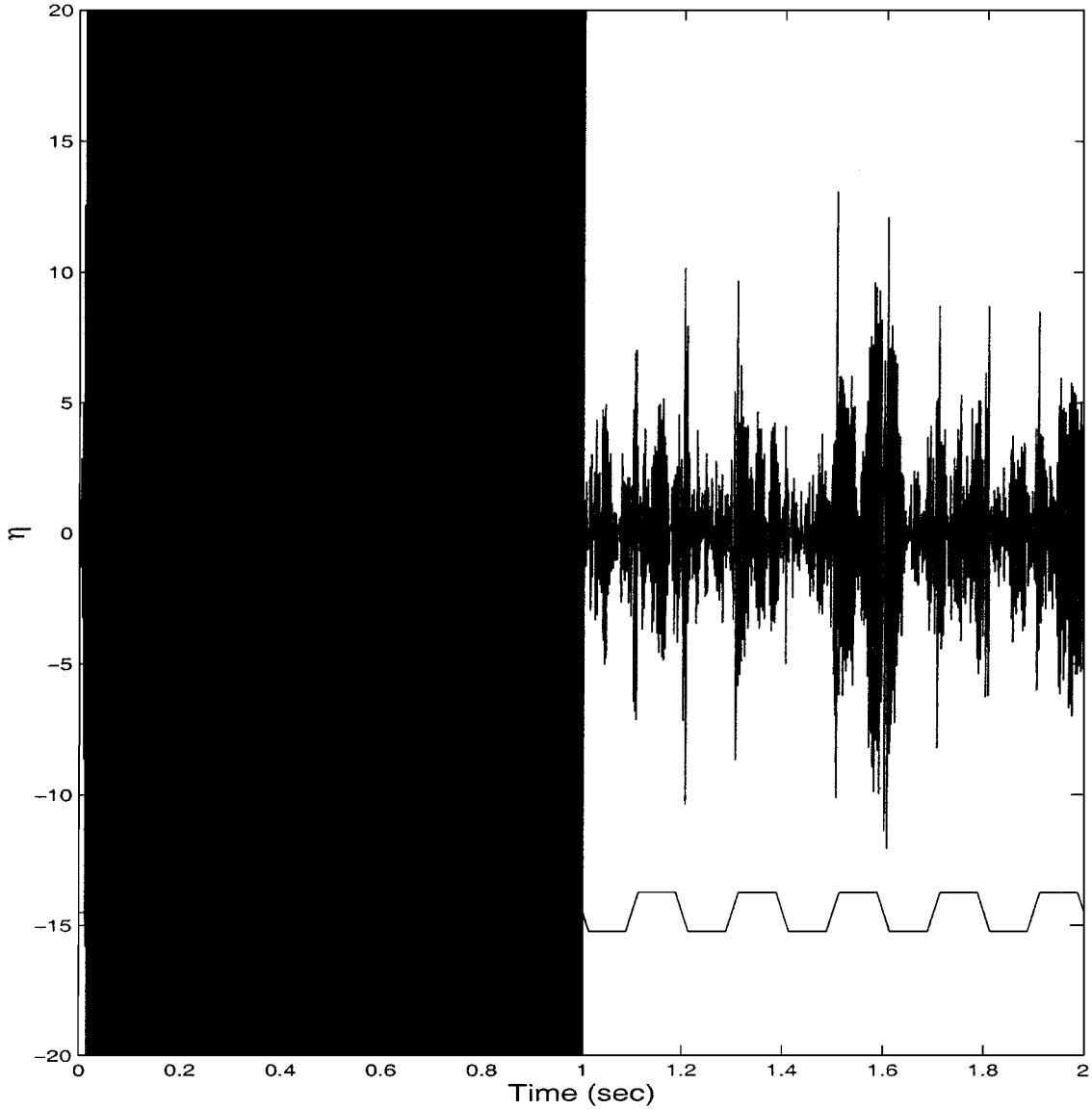

Fig. 4 Stabilizing effect of open-loop equivalence ratio modulation between two stable points. Response shown on the left half corresponds to operation at ϕ_{av}; the right half shows reduction in pressure oscillations obtained from equivalence ratio modulation. Compare with Fig. 10a of Richards et al.[17]

mechanisms are in a combustion system for the hysteresis. However, once it is detected, this paper gives guidelines for determining the number, width, and height of secondary-fuel pulses to efficiently stabilize the system.

V. Simulations

We now present numerical results to show that a combustion rig, modeled by Eq. (17), can be stabilized using an open-loop switching strategy with a nonzero transition time. The simulation model is

$$\ddot{\eta} + 2\zeta_\phi \omega_\phi \dot{\eta} + \left(\omega_\phi^2 - k_{1\phi}\right)\eta + k_{2\phi}\eta(t - \tau_\phi) = w \qquad (42)$$

where w is a process noise vector. We have added w to the system dynamics to represent the effects of unmodeled dynamics and external disturbances. This addition does not affect stability properties of the system. Numerical results are given for the stable-stable and stable-unstable switching cases corresponding to the experimental conditions in Richards et al.[17] Our results with the linear simulation model corroborate those of Richards et al.[17]

For the numerical results presented next, we used an unstable frequency ω of 300 Hz and an equivalence ratio transition time δ of 0.0125 s as in Richards et al.[17] White noise with a covariance of 200 was used as the process noise w. Initial conditions were randomly set, but the same initial state was used for simulation at desired operating point ϕ_{av} with no switching and simulation with open-loop switching strategy. Table 1 gives numerical values of other model parameters. These parameters were used to compute W_p using Eq. (32) and the smallest period $T_m^{\min}$ using the LMIs in Eq. (39), both in the stable-stable and stable-unstable switching case and are as follows:

Stable-stable nonideal switching:

$$W_p = 0.5, \qquad T_m^{\min} = 0.05$$

Stable-unstable nonideal switching:

$$W_p = 0.5, \qquad T_m^{\min} = 0.05$$

For solving the LMIs, we used $\epsilon = \delta/2$.

Table 1 Numerical values of parameters used in simulations (Equivalence ratios ϕ_1, ϕ_{av}, ϕ_2, pulse width W_p and period T_m are from Richards et al.[17]

Parameter	Stable-stable	Stable-unstable
$(\phi_1, \phi_{\text{av}}, \phi_2)$	(0.65, 0.7, 0.75)	(0.8, 0.9, 1)
$(\omega_{\phi_1}, \omega_{\phi_{\text{av}}}, \omega_{\phi_2})$	(300, 300, 300)	(300, 300, 300)
$(\zeta_{\phi_1}, \zeta_{\phi_{\text{av}}}, \zeta_{\phi_2})$	(0.05, 0, 0.01)	(0.05, 0, −0.005)
$(k_{1\phi_1}, k_{1\phi_{\text{av}}}, k_{1\phi_2})$	$(\omega_{\phi_1}, \omega_{\phi_{\text{av}}}, \omega_{\phi_2})$	$(\omega_{\phi_1}, \omega_{\phi_{\text{av}}}, \omega_{\phi_2})$
$(k_{2\phi_1}, k_{2\phi_{\text{av}}}, k_{2\phi_2})$	$(\omega_{\phi_1}, \omega^2_{\phi_{\text{av}}}, \omega_{\phi_2})$	$(\omega_{\phi_1}, \omega^2_{\phi_{\text{av}}}, \omega_{\phi_2})$
$(\tau_{\phi_1}, \tau_{\phi_{\text{av}}}, \tau_{\phi_2})$	$(\pi/\omega_{\phi_1}, 2\pi/\omega_{\phi_{\text{av}}}, \pi/\omega_{\phi_2})$	$(\pi/\omega_{\phi_1}, 2\pi/\omega_{\phi_{\text{av}}}, \pi/\omega_{\phi_2})$
(W_p, T_m)	(0.5, 0.2)	(0.5, 0.2)

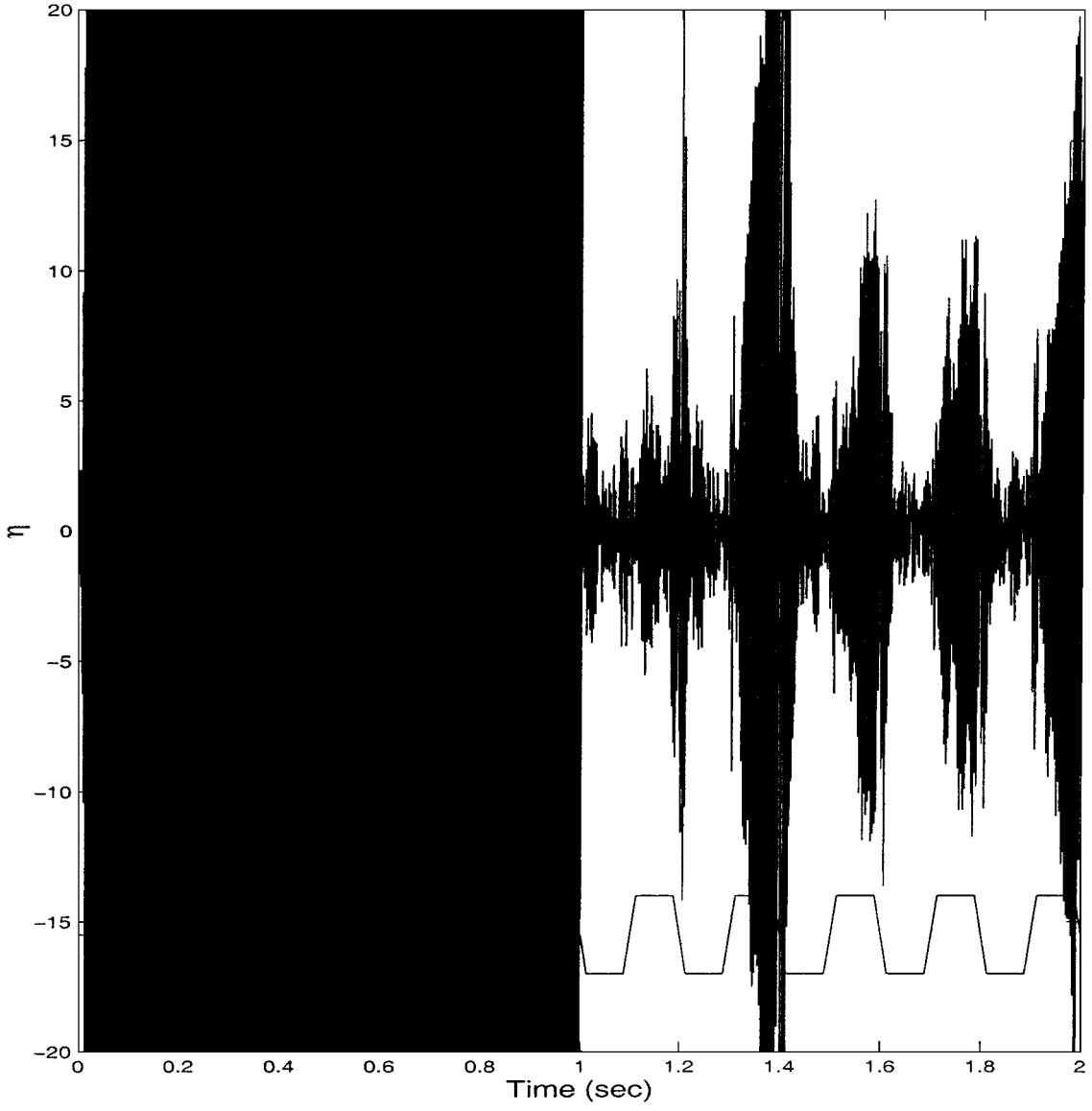

Fig. 5 Stabilizing effect of open-loop equivalence ratio modulation between a stable and an unstable point. Response shown on the left half corresponds to operation at ϕ_{av}; the right half shows response with equivalence ratio modulation. Compare with Fig. 7a of Richards et al.[17]

A. Simulation 1: Stable-Stable Switching

Here, the desired operating condition is unstable, and the strategy is to switch between two stable points "hopping over" the instability. This case corresponds to experimental results near the operating point $\phi_{av} = 0.7$ (at an inlet temperature of 367 K) presented in Richards et al.[17] Numerical values used for simulations are given in Table 1.

Figure 4 shows pressure response of the simulation model (42). The left half of the plot shows pressure response at the desired equivalence ratio ϕ_{av} with no switching. The right half of the plot shows reduction in pressure obtained with open-loop switching. The plot at the bottom shows switching sequence with nonzero transition time. It is clear that the open-loop switching strategy is stabilizing. This figure compares very well with the experimental results presented in Richards et al.[17] (see Fig. 10a therein).

B. Simulation 2: Stable-Unstable Switching

In this case the desired operating condition is unstable and is not an isolated instability as in the preceding case that allowed us to hop over to a stable operating point. This condition corresponds to the experimental results near the operating point $\phi_{av} = 0.9$ given in Richards et al.[17] and the open-loop control strategy is to switch between a stable operating point and an unstable operating point.

Figure 5 shows pressure response of the linear simulation model (42). The left half of the plot shows pressure response at the desired equivalence ratio ϕ_{av} with no switching. The right half of the plot shows the effect of open-loop switching. The large jumps in amplitude is caused by switching to an unstable operating point. The plot at the bottom shows switching sequence with nonzero transition time. As in the preceding case, this figure compares very well with the experimental results presented in Richards et al.[17] (see Fig. 7a therein).

C. Simulation 3: Evaluation of Results in Richards et al.[16]

The open-loop control strategy is evaluated at three different operating points in Richards et al.[16] The switching period is still chosen to be considerably smaller than the unstable frequency. Because the control strategy evaluated in this paper consists of slow switching, we discuss the conditions cited in Sec. III and their ability to predict the results of Richards et al.[16] as well in this section.

The minimum and maximum overall equivalence ratios used in Richards et al.[16] are $\phi_1 = 0.73$ (pulse injector off) and $\phi_2 = 0.85$ (pulse injector on). This means that, unlike the preceding cases, we can attain any desired equivalence ratio ϕ_{av} in the range $[\phi_1, \phi_2]$ by selecting an appropriate pulse width W_p according to Eq. (32). The experimental results given in Richards et al.[16] correspond to

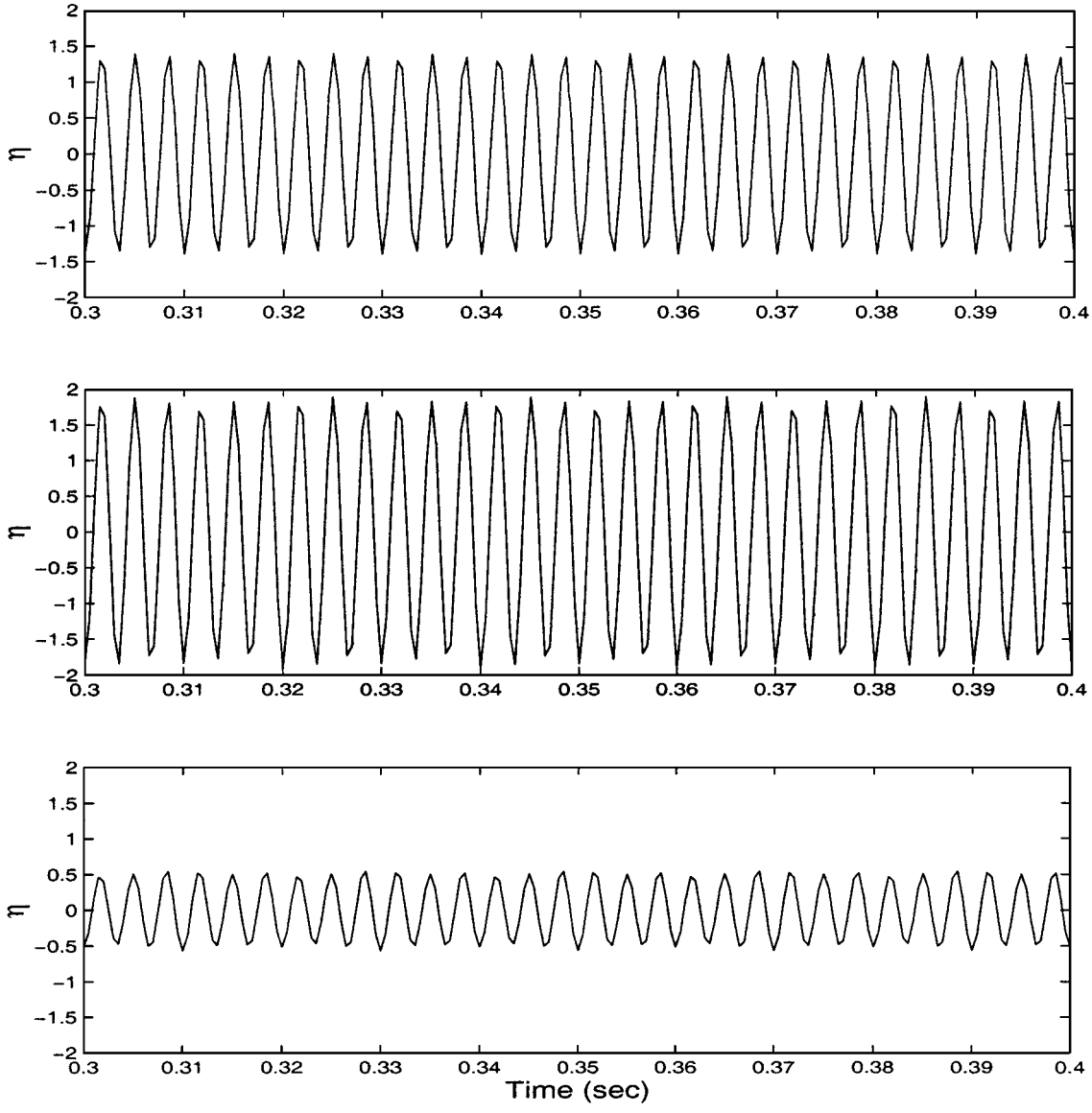

Fig. 6 Response of the linear simulation model. The top plot is for operation at $\phi_{av} = \phi_1 = 0.73$ with no switching; the middle plot is for operation at $\phi_{av} = 0.826$ with switching and a duty cycle of 80%; the bottom plot is for operation at $\phi_{av} = 0.7732$ with switching and a duty cycle of 36%. Compare with Figs. 5, 7, and 8 of Richards et al.[16]

1) $W_p = 0$, $\phi_{\text{av}} = 0.73$ (fuel injector off); 2) $W_p = 0.2$, $\phi_{\text{av}} = 0.826$ (with a duty cycle of 80%); and 3) $W_p = 0.64$, $\phi_{\text{av}} = 0.7732$ (with a duty cycle of 36%). Results in Richards et al.[16] at a switching frequency of 50 Hz ($T_m = 0.02$ s) show that pressure oscillations are slightly larger with the switching strategy 2) is applied than when the injector is off (as in 1). It is also shown in Richards et al.[16] that pressure oscillations are significantly reduced by applying the strategy 3). These observations can be explained with the same analytical developments of Sec. III with a suitable choice of the combustor model parameters.

The following values are chosen for numerical simulation:

$$\omega_\phi = 600\pi = k_{1\phi} = k_{2\phi} = \pi/\tau, \qquad \zeta_{\phi_1} = 0.01$$

$$\zeta_{0.7732} = 0.05, \qquad \zeta_{0.826} = 0.005, \qquad \zeta_{\phi_2} = 0.001$$

These choices are motivated by the experimental conditions in Richards et al.[16] A transition time of $\delta = 0.005$ s was used. The corresponding results are shown in Fig. 6. Indeed stabilization occurs in case 3), and larger oscillations are present in case 2). This is similar to the observations in Figs. 5, 7, and 8 of Richards et al.[16]

VI. Conclusions

The discussions in Secs. II–V show that an analytical model can be derived, which provides explanations and guidelines for the success of an open-loop control strategy with a large enough switching period. It was shown that an appropriate switching strategy can be found for stabilizing the combustor both while switching between two stable operating points and while switching between a stable and an unstable operating points. It was also shown that the numerical simulation studies match these analytical predictions and, more importantly, match the experimental observations in Richards et al.[16,17]

The discussions in Sec. III showed that the success of a slowly switching open-loop control strategy essentially depends on the nature of the parameter vector $f(\phi)$ defined in Eq. (20). If $f(\phi)$ belongs to one of the cases a)–c) defined in Sec. III.A.2, then $f(\phi)$ determines the feasibility of the open-loop strategy with the specific case fixing the parameters of the switching scheme (18). Therefore, a determination of how $f(\phi)$ varies with ϕ in a given rig is useful for determining the control strategy. Of the parameters $(\omega_\phi, \zeta_\phi, k_{1\phi}, \alpha_{1\phi}, \alpha_{2\phi}, \tau_\phi)$ in $f(\phi)$, the most sensitive is τ. As shown in Eq. (14), in the case when the instability mechanism is caused by variations in u', $\tau = \tau_f$; τ_f changes with the burning velocity S_u, which in turn is quite sensitive to changes in ϕ. For example, in propane-air mixture a 25% change in ϕ leads to a 400% change in S_u (Ref. 30). Also, noting the structure of Eq. (19), it is clear that changes in the time delay lead to a more drastic change in the stability pattern of the underlying system rather than changes in the other parameters of $f(\phi)$. In particular, suppose we are interested in operating conditions ϕ_1 and ϕ_2, both of which are stable and ϕ_{av} is unstable. If the dominant effect of ϕ is on τ, then the system should exhibit a stable-unstable-stable pattern as τ increases from a value that corresponds to ϕ_1, through ϕ_{av} to ϕ_2. Such stability bands are known to exist in time-delay systems in general and in the experimental rig in Richards et al.[17] in particular (Fig. 6). It is worth noting that in Richards et al.,[17] care is taken to ensure that the equivalence ratio fluctuations in the feed system are decoupled from the burning zone. It is therefore quite likely that their configuration consists of an instability mechanism where fluctuations in u' are dominant. The preceding discussions indicate that the results presented in this paper corroborate the observations in Richards et al.[17] rather closely. First, the instability properties of the uncontrolled process parallel those of the model in Eq. (13). Second, a slow switching strategy has been shown in Sec. III to lead to stability properties that are quite similar to the experimental observations in Richards et al.[17]

We have also discussed the results in Richards et al.[16] in Sec. III. This combustor differs from that in their later work[17] in two respects. First, variations in ϕ' are present in the rig. This implies that the time delay the combustor may be due to τ_c. Second, the control strategy in Richards et al.[16] was attempted at different duty cycles; this is in contrast to the later work[17] where the duty cycle was fixed at 50%, and only the values ϕ_1 and ϕ_2 between which ϕ was changed were altered. As mentioned in Secs. II and V, if the duty cycle is changed the operating point ϕ_{av} shifts. The success of the switching strategy in such a case is simply governed by the value of $f(\phi_{\text{av}})$. This is quite distinct from the strategy in Richards et al.[17] where ϕ_{av} is fixed. In fact, it can be argued that in this case, to achieve stabilization, one does not need to switch between two values in a periodic manner but could simply operate at a ϕ_{av}, based on the value $f(\phi_{\text{av}})$. If $f(\phi_{\text{av}})$ corresponds to a stable value, slow switching around this operating condition will still lead to stability, whereas switching around an unstable value of $f(\phi_{\text{av}})$ leads to a more unstable response, which might have been the cause of the observations in Figs. 7 and 8 in Richards et al.[16]

Yet another question that is raised in Richards et al.[17] is the number and location of multiple fuel injectors required to ensure the success of the proposed switching strategy. Again, this can be quantified using our model and $f(\phi)$. The ultimate goal is the realization of two values ϕ_1^* and ϕ_2^* around the desired operating point ϕ_{av} at which stability can be realized. Noting that these values correspond to the equivalence ratio at the burning section, in the situation where multiple fuel injectors are used the problem is to identify at least two choices among various sequences of pulses of fuel injector that correspond to these desired values. Suppose that there are n fuel injectors, located at n different locations, and each can, at any instant, be in the on or off mode. The sequence of pulses from these n injectors at a time instant can be expressed as $\{e_1, \ldots, e_n\}$, where each e_i can take a value 1 or 0 depending on whether the ith injector is in the on or off mode. Hence, it follows that 2^n possible sequences S_i can be generated using these n fuel injectors. The issue is therefore to identify the mapping from S_i to ϕ_i and find the S_i that correspond to the desired ϕ_1^* and ϕ_2^*. In general, these sequences are bound to depend in a complex way on the configuration and boundary conditions in a given rig. Once these sequences are identified, they determine in turn when a given injector is fired. Given the quasi-static nature of the switching strategy (that is, the switching frequency is significantly smaller than the unstable frequency), the time delay between the firing instants of any two injectors might not be a relevant parameter as was speculated by Richards.[18]

We have also showed in this paper an explanation for when and how a combustor can be stabilized using a switching strategy in the presence of hysteresis.[20,21] In particular, we have shown that the same proposition that explained the idea behind stabilization using the switching strategy in Richards et al.[16,17] provides the analytical basis for results in the presence of hysteresis. We showed that our observations based on the model and the proposition matches the experimental observations.[20,21]

A point worth making is about properties of open-loop control strategies in general. Unlike closed-loop control strategies, open-loop control strategies are quite vulnerable to changes in the operating parameters. As the preceding discussion indicated, the stability of the open-loop strategy is closely tied to $f(\phi)$, and hence its stability robustness is conditioned on the sensitivity of $f(\phi)$ to various perturbations and changes in the operating conditions. This should be kept in mind while implementing open-loop control strategies. For the switching strategy in Eq. (18), stability depends only on $f(\phi_1)$ and $f(\phi_2)$ and not on how the function f behaves at other values of ϕ.

Finally, we make a comment about the model in Eq. (17), which is a second-order, lumped, time-delay model. Obviously, a fair amount of simplification has been made in collapsing the complex dynamic interactions between acoustic modes, heat-release dynamics from a distributed flame zone, fuel injection, and mixing dynamics into a simple form. However, the description of the open-loop control strategy and its impact on the rig using the time-delay model as in Eq. (17) represents a very useful guideline and an important beginning for how the physical model can be expanded appropriately to encompass various dynamics exhibited by a combustion rig with and without active control.

Acknowledgments

This work is sponsored in part by the National Science Foundation, Contract ECS 9713415, and in part by the Office of Naval Research, Contract N00014-99-1-0448.

References

[1]Heckl, M. A., "Active Control of the Noise from a Rijke Tube," *Aero- and Hydro-Acoustics*, edited by G. Comte-Bellot and J. E. Flowers Williams, Springer, Berlin, 1986, pp. 211–216.

[2]Lang, W., Poinsot, T., and Candel, S., "Active Control of Combustion Instability," *Combustion and Flame*, Vol. 70, No. 3, 1987, pp. 281–289.

[3]Bloxsidge, G. J., Dowling, A. P., Hooper, N., and Langhorne, P. J., "Active Control of an Acoustically Driven Combustion Instability," *Journal of Theoretical and Applied Mechanics*, Vol. 6, 1987, pp. 161–175.

[4]Poinsot, T., Bourienne, F., Candel, S., and Esposito, E., "Suppression of Combustion Instabilities by Active Control," *Journal of Propulsion and Power*, Vol. 5, No. 1, 1989, pp. 14–20.

[5]Langhorne, P. J., Dowling, A. P., and Hooper, N., "Practical Active Control System for Combustion Oscillations," *Journal of Propulsion and Power*, Vol. 6, No. 3, 1990, pp. 324–333.

[6]Gulati, A., and Mani, R., "Active Control of Unsteady Combustion-Induced Oscillations," *Journal of Propulsion and Power*, Vol. 8, No. 5, 1992, pp. 1109–1115.

[7]McManus, K. R., Vandsburger, U., and Bowman, C. T., "Combustor Performance Enhancement Through Direct Shear Layer Excitation," *Combustion and Flame*, Vol. 82, No. 1, 1990, pp. 75–92.

[8]Gutmark, E., Parr, T. P., Wilson, K. J., Hanson-Parr, D. M., and Schadow, K. C., "Closed-Loop Control in a Flame and a Dump Combustor," *IEEE Control Systems*, Vol. 13, No. 2, April 1993, pp. 73–78.

[9]Annaswamy, A. M., Fleifil, M., Hathout, J. P., and Ghoniem, A. F., "Impact of Linear Coupling on the Design of Active Controllers for Thermoacoustic Instability," *Combustion Science and Technology*, Vol. 128, No. 1–6, Dec. 1997, pp. 131–180.

[10]Fleifil, M., Hathout, J. P., Annaswamy, A. M., and Ghoniem, A. F., "The Origin of Secondary Peaks with Active Control of Thermoacoustic Instability," *Combustion Science and Technology*, Vol. 133, No. 4–6, 1998, pp. 227–265.

[11]Hathout, J. P., Annaswamy, A. M., Fleifil, M., and Ghoniem, A. F., "A Model-Based Active Control Design for Thermoacoustic Instability," *Combustion Science and Technology*, Vol. 132, No. 1–6, May 1998, pp. 99–138.

[12]Annaswamy, A. M., El-Rifai, O., Fleifil, M., and Ghoniem, A. F., "A Model-Based Self-Tuning Controller for Thermoacoustic Instability," *Combustion Science and Technology*, Vol. 135, Aug. 1998, pp. 213–240.

[13]Neumeier, Y., and Zinn, B. T., "Active Control of Combustion Instabilities Using Real Time Identification of Unstable Combustor Modes," *Proceedings of the IEEE Conference on Control Applications*, Albany, NY, 1995, pp. 691–698.

[14]Tierno, J. E., and Doyle, J. C., "Multimode Active Stabilization of a Rijke Tube," *DSC*, Vol. 38, 1992.

[15]Murugappan, S., Park, S., Annaswamy, A. M., Gutmark, E., Ghoniem, A. F., Acharya, S., and Algood, T., "Optimal Control of Swirl-Stabilized Combustor Using a System Identification Based Model," *Turbine 2000*, 2000.

[16]Richards, G. A., Yip, M. C., Robey, E., Cowell, L., and Rawlins, D., "Combustion Oscillation Control by Cyclic Fuel Injection," *Journal of Engineering for Gas Turbines and Power*, Vol. 119, No. 2, 1997, pp. 340–343.

[17]Richards, G. A., Janus, M., and Robey, E. H., "Control of Flame Oscillations with Equivalence Ratio Modulation," *Journal of Propulsion and Power*, Vol. 15, No. 2, 1999, pp. 232–240.

[18]Richards, G. A., "Methods to Control Combustion Dynamics," *AGTSR Workshop*, 1999.

[19]Brouwer, J., Ault, B. A., Bobrow, J. E., and Samuelsen, G. S., "Active Control for Gas Turbine Combustors," *Twenty-Third Symposium (International) on Combustion*, Combustion Inst., Pittsburgh, PA, 1990.

[20]Knoop, P., Culick, F. E. C., and Zukoski, E. E., "Extension of the Stability of Motions in a Combustion Chamber by Nonlinear Active Control Based on Hysteresis," *Short Communication, Combustion Science and Technology*, Vol. 123, No. 1–6, 1997, pp. 363–376.

[21]Isella, G., Seywert, C., Culick, F. E. C., and Zukoski, E. E., "A Further Note on Active Control of Combustion Instabilities Based on Hysteresis," *Short Communication, Combustion Science and Technology*, Vol. 126, No. 1–6, 1997, pp. 381–388.

[22]Najm, H. M., and Ghoniem, A. F., "Modeling Pulsating Combustion in Vortex Stabilized Pre-Mixed Flames," *Short Communication, Combustion Science and Technology*, Vol. 94, No. 1–6, 1993, pp. 259–278.

[23]Fleifil, M., Annaswamy, A. M., Ghoniem, Z., and Ghoniem, A. F., "Response of a Laminar Premixed Flame to Flow Oscillations: A Kinematic Model and Thermoacoustic Instability Result," *Combustion and Flame*, Vol. 106, No. 4, 1996, pp. 487–510.

[24]Hathout, J. P., Fleifil, M., Annaswamy, A. M., and Ghoniem, A. F., "Active Control of Combustion Instability Using Fuel-Injection in the Presence of Time-Delays," *Journal of Propulsion and Power*, Vol. 18, No. 2, 2002, pp. 390–399.

[25]Dowling, A. P., and Ffowcs-Williams, J. E., *Sound and Sources of Sound*, Ellis Horwood Limited, West Sussex, England, 1983.

[26]Yang, V., and Anderson, W. (eds.), *Liquid Rocket Engine Combustion Instability*, Progress in Astronautics and Aeronautics, AIAA, Washington, DC, 1995.

[27]Peracchio, A. A., and Proscia, W., "Nonlinear Heat Release/Acoustic Model for Thermoacoustic Instability in Lean Premixed Combustors," *ASME Gas Turbine and Aerospace Congress*, 1998.

[28]Boyd, S. P., El Ghaoui, L., Feron, E., and Balakrishnan, V., *Linear Matrix Inequalities in Systems and Control Theory*, Society for Industrial and Applied Mathematics, Philadelphia, PA, 1994.

[29]Desoer, C. A., and Vidyasagar, M., *Feedback Systems: Input-Output Properties*, Academic Press, New York, 1975.

[30]Williams, F. A., *Combustion Theory*, Addison Wesley Longman, Reading, MA, 1965.